Romanian Reports in Physics, Vol. 67, No. 2, P. 500–507, 2015

OPTICS

PROPAGATION CHARACTERISTICS IN A NEW PHOTONIC FIBER–BASED PLASMONIC SENSOR

V. A. POPESCU*, N. N. PUSCAS

"Politehnica" University of Bucharest, Department of Physics 1, Splaiul Independentei 313, 060042 Bucharest, Romania
*Corresponding author: vapopescu@yahoo.com

Received June 12, 2014

Abstract. The propagation characteristics in a new photonic fiber-based plasmonic sensor are investigated using a finite element method. The fiber is made by a SiO_2 core in the center of the structure, a GaP reflector layer with high refractive index, a SiO_2 reflector layer which is surrounded by a gold layer and a very thickness distilled water layer. In this sensor there is a strong interaction between the core and plasmon modes near the loss matching point in the visible part of the spectrum. The advantages of this configuration are a higher amplitude sensitivity, a smaller propagation length and a better value of the detection limit of the amplitude-based sensor.

Key words: sensors, surface plasmons, fiber optics sensors.

1. INTRODUCTION

An extensive variety of microstructured and photonic fiber-based plasmonic sensors with broad applications in detection of changes in the refractive index of an analyte have been analysed [1–12]. In two recently papers [1–2], a solid core Bragg fiber-based surface plasmon resonance sensor for detection in aqueous analytes has been analysed. This sensor is made by a core with a low refractive index which is surrounded by a number of alternating high and low refractive index reflector layers and by a thin gold layer which is deposited on the outer surface in contact with an analyte layer. The thicknesses of the reflector layer are given by the quarter wave condition to assurance the destructive interference of guided light in the periodic fiber cladding and an efficient modal confinement in the fiber hollow core. However, in this case the loss at the phase matching point is only 6 dB/cm for an analyte refractive index of 1.33.

The proposed photonic plasmon optical fiber-based plasmonic sensor (Fig. 1) with a very high light absorption at the loss matching point (in the place of the phase matching point from [1]), includes a SiO_2 core in the center of the structure,

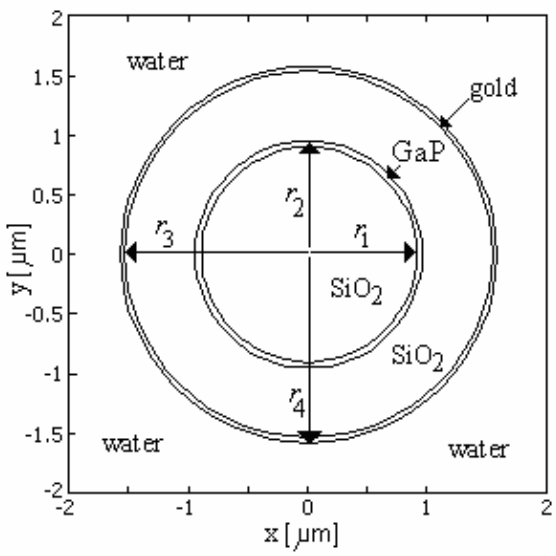

Fig. 1 – Cross section of a photonic fiber made by a SiO_2 core (radius r_1) in the center of the structure, a GaP layer with high refractive index (thickness $r_2 - r_1$), a SiO_2 layer (thickness $r_3 - r_2$) which is surrounded by a gold layer (thickness $r_4 - r_3$) and a very thickness distilled water layer.

a GaP reflector layer with high refractive index, a SiO_2 reflector layer which is surrounded by a thin gold layer that can be assumed as a partial reflector layer and a very thickness distilled water layer. A finite element method is used to compute the propagation constants of the core and plasmon modes in the structure and to analyze the power absorption efficiency for these modes.

2. PHOTONIC FIBER–BASED PLASMONIC SENSOR

The proposed photonic optical fiber (Fig. 1) is made by a SiO_2 core (radius r_1) in the center of the structure, a GaP reflector layer with high refractive index (thickness $r_2 - r_1$), a SiO_2 reflector layer (thickness $r_3 - r_2$) which is surrounded by a thin gold layer (thickness $r_4 - r_3$) and a very thickness distilled water layer. Each layer boundary produces a partial reflection of an optical wave and for a wave where the wavelength is close to four times the optical thickness of the layers, the many reflections combine with constructive interference, and the layers act as a reflector. In our case the boundaries between the SiO_2 and GaP layers and between the gold and water, causes a shift phase of 180^o because the incident light goes from low- index medium in a high- index medium. Thus, the relative phase difference of all reflected waves is zero or a multiple of 360^o, and consequently an efficient modal confinement in the fiber hollow core.

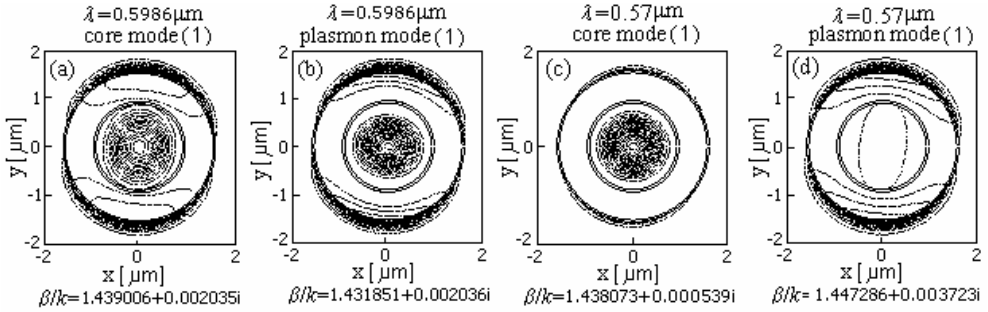

Fig. 2 – Contour plot of the z-component $S_Z(x, y)$ of the Poynting vector at the resonance (λ = 0.5986 μm) between the guided (a) and the plasmon (b) modes and also for the guided (c) and plasmon (d) modes at a considerable distance (λ = 0.57 μm) from the loss matching point in a photonic fiber with a single gold layer. For a core mode and λ < 0.5986 μm, the main electric field orientation is in the same sense in the SiO_2 core and in the water layer but for λ > 0.5986 μm, the orientations of these fields are antiparallel. For a plasmon mode, the orientations of these fields are in the opposite direction in comparison with that of the core mode.

The wavelength dependence of the refractive index of the silica [13–15], distilled water [16], gold [13–14, 17], heavy water [18] and GaP [19] has been modeled by using a Sellmeier formula for SiO_2, H_2O, D_2O and GaP or a Drude relation for Au. The continuity conditions require that the tangential components of the electric field E and the magnetic field H are matched at the different layer interfaces, whereas the complex propagation constant $\beta = \beta_r - j\beta_i$ for each mode is determined from the dispersion equation. The power fraction in different part of the structure is determined by using the z-component of the Poynting vector. The intensity of the surface plasmon wave decays with the square of the electric field and the propagation length $L = 1/(2\beta_i)$ is defined as the distance for the intensity to decrease by a factor of 1/e. The losses in dB/cm are defined as $\alpha = 400{,}000\pi\ \beta_i / (k\lambda \ln(10))$, where λ is in μm and k is the vacuum wavenumber. The amplitude sensitivity $S_A(\lambda)$, the group refractive index n_g and the group velocity v_g are defined [8–10] in function of the effective index $n_{eff} = \beta/k$.

3. NUMERICAL RESULTS AND DISCUSSION

A finite element method [8, 9, 20] is used to compute the propagation constants of the core and plasmon modes in a photonic fiber. Figure 1 shows a cross section of a photonic fiber made by a SiO_2 core (radius r_1 = 0.9 μm) in the center of the structure, a GaP reflector layer with high refractive index (thickness $r_2 - r_1$ = 52.534 nm), a SiO_2 reflector layer (thickness $r_3 - r_2$ = 583.33 nm) which is surrounded by a gold layer (thickness $r_4 - r_3$ = 40 nm) and a very thickness distilled water layer. The fundamental core mode of this sensor structure is a two-fold

degenerate core mode where, at large distance from the resonant wavelength, the real parts of effective indices are equal for two components of the degenerate core mode but the main electric field orientation perpendicular to each other, respectively.

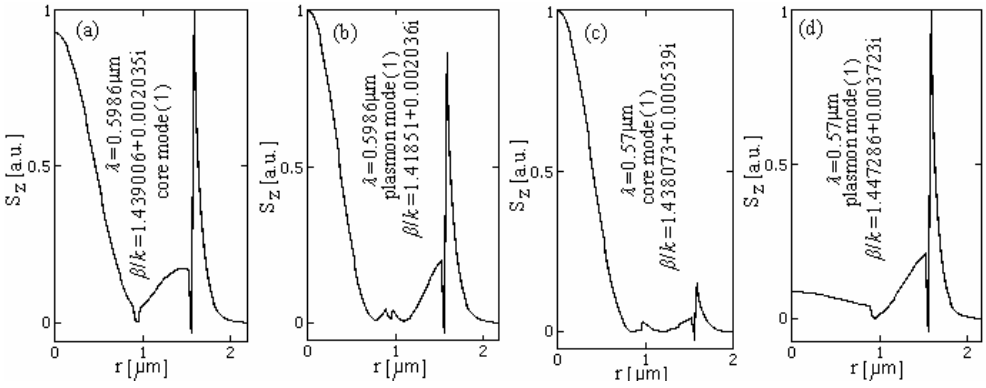

Fig. 3 – Radial (positive *y*-direction) cross section of the z-component $S_Z(x, y)$ of the Poynting vector near the resonance (λ = 0.5986 μm) between the guided (a) and the plasmon (b) modes and also for the guided (c) and plasmon (d) modes at a considerable distance (λ = 0.57 μm) from the loss matching point in a photonic fiber.

Table 1

The power fraction carried in the distilled water (or heavy water), gold, SiO_2 exterior, SiO_2 interior and GaP layers by the core and plasmon modes at the loss matching point (λ = 0.5986 μm for H_2O and λ = 0.5825 μm for D_2O) and at a considerable distance (λ = 0.57 μm) from the loss matching point in H_2O

λ [μm]	H_2O (D_2O) core plasmon	Gold core plasmon	SiO_2 ext. core plasmon	SiO_2 int. core plasmon	GaP core plasmon
0.5986 (H_2O)	0.304806 0.342997	0.008025 0.009435	0.196101 0.156150	0.490574 0.489245	0.000494 0.002173
0.5825 (D_2O)	0.335478 0.305284	0.010174 0.008930	0.157647 0.202011	0.494862 0.483261	0.001840 0.000513
0.5700 (H_2O)	0.090648 0.538887	0.003220 0.018091	0.055917 0.310459	0.848765 0.131938	0.001449 0.000626

Figure 2 shows the contour plot of the *z*-component $S_Z(x, y)$ of the Poynting vector at the resonance (λ = 0.5986 μm) between the first (1) of twofold degenerate core guided mode and the corresponding plasmon mode and also for the core and plasmon modes at a considerable distance (λ = 0.57 μm) from the loss matching point in a photonic fiber. The difference (0.000001) between the imaginary parts of the effective indices of core mode and plasmon mode is the smallest at the loss matching point (λ = 0.5986 μm) where β/*k* = 1.439006 + 0.002035i for the core mode and β/*k* = 1.431851 + 0.002036i for the plasmon mode. For a core mode and

$\lambda < 0.5986$ μm, the main electric field orientation is in the same sense in the SiO_2 core and in the water layer but for $\lambda > 0.5986$ μm, the orientations of these fields are antiparallel. For a plasmon mode, the orientations of these fields are in the opposite direction in comparison with that of the core mode.

Figure 3 reports a radial (positive *y*-direction) cross section of the *z*-component $S_Z(x, y)$ of the Poynting vector near the resonance ($\lambda = 0.5986$ μm) between the guided and the plasmon modes and also for the guided and plasmon modes at a considerable distance ($\lambda = 0.57$ μm) from the loss matching point in the same photonic fiber. It can be noted that at shorter wavelengths, where there is no resonance effect, both the core guided mode and the plasmon mode are well confined, while near the loss matching point ($\lambda = 0.5986$ μm) a large portion of the energy penetrates into the metal from the core mode and the two modes are strongly coupled. For a decrease Δn_a of the analyte refractive index by 0.00410692 RIU ($n_a = 1.3325796127$ at $\lambda = 0.5986$ μm for H_2O and $n_a = 1.32847269$ at $\lambda = 0.5825$ μm for D_2O), the loss matching point for the core mode is shifted by 16.1 nm towards shorter wavelengths, with a spectral resolution of 2.6×10^{-5} RIU (assuming a spectral resolution of 0.1 nm).

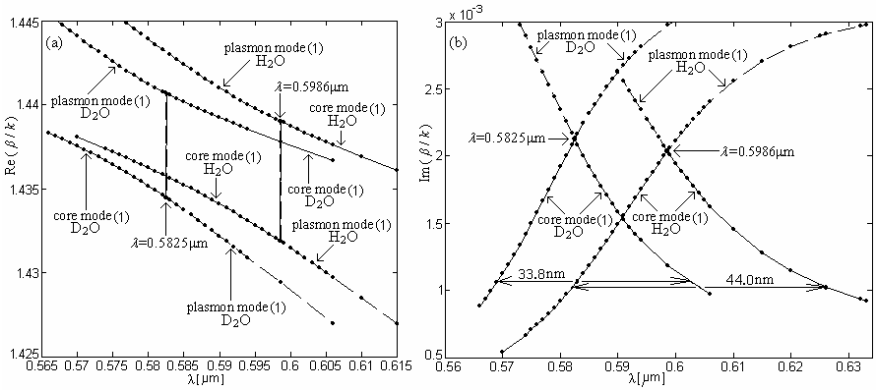

Fig. 4 – The real (a) and imaginary (b) parts of the effective index *versus* the wavelength for the core mode and the corresponding plasmon mode near the loss matching point ($\lambda = 0.5986$ μm for H_2O and $\lambda = 0.5825$ μm for D_2O) in a photonic fiber. The full width at half maximum (FWHM) bandwidth for the guided mode is 44.0 nm (33.8 nm for a symmetric line shape) for distilled water and 33.8 nm (26.8 nm for a symmetric line shape) for the heavy water.

Figure 4 shows the real and imaginary parts of the effective index *versus* the wavelength for the core mode and the corresponding plasmon mode near the loss matching point ($\lambda = 0.5986$ μm for H_2O and $\lambda = 0.5825$ μm for D_2O) in a photonic fiber. The full width at half maximum (FWHM) bandwidth for the guided mode is 44.0 nm (33.8 nm for a symmetric line shape) for distilled water and 33.8 nm (26.8 nm for a symmetric line shape) for the heavy water. It is important to note a large difference (10 nm) between these bandwidths. Then, the signal-to-noise ratio for

the core mode is SNR = $\delta\lambda_{res}/\delta\lambda_{0.5}$ = 3.9 nm/44.0 nm ≈ 0.09 when the analyte is a distilled water, and SNR = $\delta\lambda_{res}/\delta\lambda_{0.5}$ = 3.9 nm/33.8 nm ≈ 0.12 when the analyte is a D_2O layer. In our fiber structure (Table 1), the power fraction for the core mode in the distilled and heavy water layers is large (0.304806 for H_2O and 0.335478 for D_2O) near the loss matching point where the field of a core guided mode contains strong plasmonic contribution. Also, the power fraction in the gold layer is 0.00802499 in H_2O and 0.01017400 in D_2O for the same mode. It is interesting to note that at shorter wavelengths (λ = 0.57 μm), where there is no resonance effect, a very small portion of the power fraction for the core mode penetrates into the analyte (0.0906484 in H_2O) and metal (0.00321984 in gold) layers. For the loss matching point (λ = 0.5986 μm for H_2O and λ = 0.5825 μm for D_2O), the transmission loss (Table 2) of the guided mode is very large (1855.3 dB/cm for H_2O and 1990.9 dB/cm for D_2O). Also, the propagation length of the same mode at the resonance wavelength is only 23.4 μm for H_2O and 21.8 μm for D_2O. The maximum value of the amplitude sensitivity S_A (Fig. 5) for the guided mode (Fig. 5a) in the vicinity of 0.569 μm is 1825.5 RIU^{-1} for D_2O and near 0.578 μm is 1663.7 RIU^{-1} for H_2O. It is a typically safe assumption [7, 8] that a 1 % change in the transmitted intensity can be detected, which leads to a sensor resolution of 5.5×10^{-6} RIU for D_2O and 6.0×10^{-6} RIU for H_2O. The real part of the group refractive index n_g shows a minimum value (Fig. 5b) and the imaginary part of n_g indicates a very small value (Fig. 5c) near the loss matching point at λ = 0.582 μm for D_2O and at λ = 0.598 μm for H_2O. The difference between the wavelength for maximal amplitude sensitivity and for the resonant wavelength is small (13.5 nm for D_2O and 20.6 nm for H_2O) in comparison with 30 nm [1].

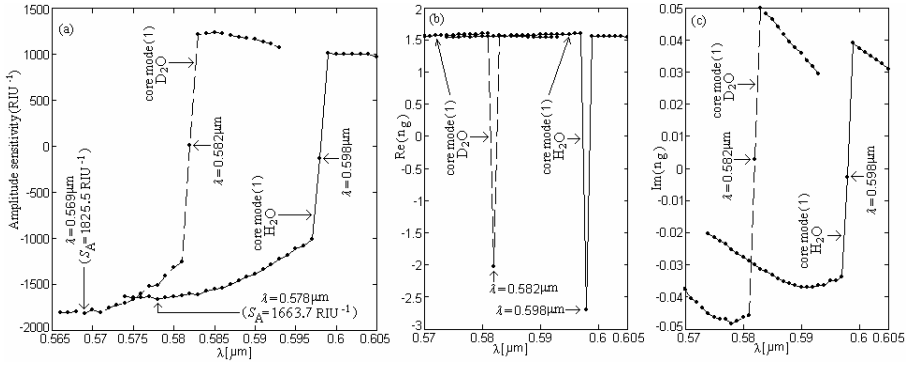

Fig. 5 – Amplitude sensitivity (a) and the real (b) and imaginary (c) parts of the group refractive index n_g for the guided mode *versus* the wavelength near the loss matching point (λ = 0.5986 μm for H_2O and λ = 0.5825 μm for D_2O) in a photonic fiber.

For another photonic fiber with r_1 = 0.9 μm for SiO_2 core, r_2 = 0.953 μm (thickness of the GaP layer $r_2 - r_1$ = 53 nm), r_3 = 1.54 μm (thickness of the SiO_2 reflector layer $r_3 - r_2$ = 587 nm), r_4 = 1.58 μm (thickness of the gold layer $r_4 - r_3$ =

= 40 nm), the difference (0.000000) between the imaginary parts of the effective indices of core mode and plasmon mode is the smallest at the loss matching point (λ_r = 0.5988 μm) where β/k = 1.439170 + 0.002037i for the core mode, and β/k = = 1.439025 + 0.002037i for the plasmon mode. The values of the thicknesses for GaP (53 nm), SiO_2 (587 nm) and gold (40 nm) layers are a good approximation to the calculated values (49 nm for GaP, 638 nm for SiO_2 and 40 nm for gold) from the relation where the resonant wavelength is four times the optical thickness of the layers. In this photonic fiber, if we increase the r_1 radius with 1 nm then the loss matching point λ_r decreases with 0.2 nm, if increase the thickness of the GaP with 1 nm then λ_r decreases with 0.2 nm, if increase the thickness of the SiO_2 exterior with 1 nm then λ_r increases with 0.1 nm and if increase the thickness of the gold layer with 1 nm then λ_r increases with 5 nm.

Table 2

Values of $\delta\lambda_{res}$ [nm], $\delta\lambda_{0.5}$ [nm], SNR, S_λ [nmRIU^{-1}], SR_λ [RIU], S_A [RIU^{-1}], SR_A [RIU], α [dB/cm], L [μm] and λ [μm], (the better results are written with bold character)

$\delta\lambda_{res}$	$\delta\lambda_{0.5}$	SNR	S_λ	SR_λ	S_A	SR_A	α	L	λ	
3.9	44.0	0.09	3920	2.6×10^{-5}	1663.7	6.0×10^{-6}	1855.3	23.4	0.5986	H_2O
3.9	33.8	0.12	3920	2.6×10^{-5}	1825.5	5.5×10^{-6}	1990.9	21.8	0.5825	D_2O
10.0	large		**10000**	**9.8×10^{-6}**	293	3.4×10^{-5}	6	10^4	0.758	[1]

Table 2 makes a comparison of the parameters for two photonic optical fiber-based surface plasmon resonance sensors such as the shift $\delta\lambda_{res}$ towards longer wavelengths of the phase matching point or loss matching point for an increase Δn_a of the analyte refractive index by 0.001 RIU, the resonance spectral width $\delta\lambda_{0.5}$ computed at the full width at half maximum (FWHM) of the loss spectra, the signal-to-noise ratio SNR, the spectral sensitivity S_λ, the spectral resolution SR_λ (detection limit in the wavelength interrogation mode), the amplitude sensitivity S_A, the sensor resolution SR_A (detection limit of the amplitude-based sensor) the loss α, the propagation length L and the wavelength λ corresponding to the loss matching point.

4. CONCLUSIONS

In the proposed photonic fiber-based plasmonic sensor there is a strong interaction between the core and plasmon modes near the loss matching point (λ = 0.5896 μm for H_2O and λ = 0.5825 μm for D_2O) in the visible part of the spectrum. The advantages of the this configuration are a higher amplitude sensitivity (1663.7 RIU^{-1} for H_2O and 1825.5 RIU^{-1} for D_2O), a higher loss (1855.3 dB/cm for

H_2O, 1990.9 dB/cm for D_2O), a smaller propagation length (23.4 μm for H_2O and 21.8 μm for D_2O) and a better value of the detection limit of the amplitude-based sensor (6.0×10^{-6} RIU for H_2O and 5.5×10^{-6} RIU for D_2O). Also, in our configurations with a small number of reflectors, the loss at the resonance is very large in comparison with 6 dB/cm [1–2] for an analyte refractive index of 1.33. The performances of our fiber sensor can be improved if replace only the GaP reflector with a gold layer [21].

REFERENCES

1. M. Skorobogatiy, J. Sens. **524237**, 1 (2009).
2. B. Gauvreau, A. Hassani, M. Fassi Fehri, A. Kabashin and M. Skorobogatiy, Opt. Express, **15**, 11413 (2007).
3. B. Shuai, L. Xia, Y. Zhang and D. Liu, Opt. Express, **20**, 5974 (2012).
4. A. Hassani and M. Skorobogatiy, Opt. Express, **14**, 11616 (2006).
5. J. Homola, Chem. Rev., **108**, 462 (2008).
6. A. Hassani and M. Skorobogatiy, J. Opt. Soc. Am. B, **24**, 1423 (2007).
7. Y. Zhang, L. Xia, C. Zhou, X. Yu, H. Liu, D. Liu, and Y. Zhang, Opt. Commun., **284**, 4161 (2011).
8. V. A. Popescu, N. N. Puscas and G. Perrone, J. Opt. Soc. Am. B, **29**, 3039 (2012).
9. V. A. Popescu, Mod. Phys. Lett. B, **26**, 1250207 (2012).
10. V. A. Popescu, Mod. Phys. Lett. B, **27**, 1350038 (2013).
11. V. A. Popescu, N. N. Puscas and G. Perrone, Eur. Phys. J. D., **67**, *1*, 215 (2013).
12. V. A. Popescu, N. N. Puscas and G. Perrone, J. Opt. Soc. Am. B, **31**, 1062 (2014).
13. A. K. Sharma, Rajan and R. B. D.Gupta, Opt. Commun., **274**, 320 (2007).
14. R. K. Verma, A. K. Sharma and B. D.Gupta, Opt. Commun., **281**, 1486 2008.
15. A. K. Ghatak and K. Thyagarajan, *Introduction to Fiber Optics*, Cambridge University Press, 1999.
16. M. Daimon and A. Masumura, Appl. Opt., **46**, 3811 (2007).
17. M. A. Ordal, L. L. Long, R. J. Bell, S. E. Bell, R. R. Bell, R. W. Alexander Jr. and C.A. Ward, Appl. Opt., **22**, 1099 (1983).
18. H. Odhner and D. T. Jacobs, J. Chem. Eng. Data, **57**, 166 (2012).
19. F. L. Madarasz, J. O. Dimmock, N. Dietz and K. L. Bachmann, J. Appl. Phys., **87**, 1564 (2000).
20. V. A. Popescu, J. Supercond. Nov. Magn., **25**, 1–6 (2012).
21. V. A. Popescu, N. N. Puşcaş and G. Perrone, J. Opt. Soc. Am., **B 32**, 473 (2015).